Matrix Infrared Spectra and Density Functional Theory Calculations of Molybdenum Hydrides

Xuefeng Wang and Lester Andrews*

Department of Chemistry, University of Virginia, McCormick Road, P.O. Box 400319, Charlottesville, Virginia 22904-4319

Received: June 30, 2005; In Final Form: August 8, 2005

Laser-ablated Mo atoms react with H_2 upon condensation in excess argon, neon, and hydrogen. The molybdenum hydrides MoH, MoH_2, MoH_4, and MoH_6 are identified by isotopic substitution (H_2, D_2, HD, $H_2 + D_2$) and by comparison with vibrational frequencies calculated by density functional theory. The MoH_2 molecule is bent, MoH_4 is tetrahedral, and MoH_6 appears to have the distorted trigonal prism structure.

Introduction

Group 6 complexes with dihydrogen have played a central role in the understanding of transition metal-dihydrogen bonding. The stable $M(CO)_3(PR_3)(H_2)$ complexes were discovered first, and the related $M(CO)_5(H_2)$ complexes were prepared by H_2 exchange with CO in low-temperature matrixes at almost the same time.[1−3] Investigations of such low-temperature stable H_2 complexes have continued to complement studies of the stable complexes.[4−10] In addition ligated MoH_2 complexes have been observed to isomerize between MoH_2 and $Mo(H_2)$ forms and to eliminate H_2 on photolysis.[10−12]

The dihydrides of group 6 metals have been observed in solid neon, argon and krypton matrixes.[13−17] In neon where more diffusion of the dihydrogen reagent occurs during sample deposition, the higher hydrides $(H_2)CrH_2$, $(H_2)CrH_2(H_2)$, WH_4, and WH_6 have been characterized.[15−17] Theoretical calculations predict that the $(H_2)CrH_2$ complex is more stable than CrH_4.[17,18] The structure of WH_6 is of particular interest as VSEPR theory suggests an octahedral structure whereas electronic structure calculations predict a distorted trigonal prismatic structure.[19−22] The recent observation of four W−H stretching fundamentals for WH_6 in solid neon, which are in excellent agreement with frequencies predicted by theory for this C_{3v} structure, confirms this characterization of the important WH_6 molecule.[15,16]

The above markedly different structures for the tetrahydrides and hexahydrides of Cr and W immediately bring into question the molybdenum counterpart structures. The following matrix-isolation experimental and density functional theoretical investigation of Mo and H_2 reaction products was performed to answer this question.

Experimental and Computational Methods

The experimental approach for reactions of laser-ablated metal atoms with small molecules during condensation in excess argon, neon, and hydrogen has been described previously.[23−25] The Nd:YAG laser fundamental (1064 nm, 10 Hz repetition rate with 10 ns pulse width) was focused onto a rotating molybdenum target (Johnson-Matthey, 99.95%) using laser energies of 5−30 mJ/pulse. Laser-ablated molybdenum atoms were co-deposited with hydrogen molecules (0.2 to 6%) in excess neon or argon or pure hydrogen (deuterium) onto a 3.5 K CsI cryogenic window at 2−3 mmol/h for 1 h using a Sumitomo Heavy Industries Model RDK-205D cryocooler. Hydrogen (Matheson), D_2, HD (Cambridge Isotopic Laboratories), and $H_2 + D_2$ mixtures were used in different experiments. FTIR spectra were recorded at 0.5 cm^{-1} resolution on a Nicolet 750 instrument with 0.1 cm^{-1} accuracy using a HgCdTe detector. Matrix samples were annealed at different temperatures, and selected samples were irradiated by a medium-pressure mercury arc street lamp (Philips, 175W) with the globe removed.

Density functional theoretical calculations of molybdenum hydrides and molybdenum hydride dihydrogen complexes were done for comparison with experiment. The Gaussian 98 program[26] was employed to calculate the structures and frequencies of expected molecules using the BPW91 and B3LYP functionals.[27−30] The 6-311++G(d,p) basis set for hydrogen and Los Alamos ECP plus DZ and SDD pseudopotentials for molybdenum atom were used.[31−33] All the geometrical parameters were fully optimized and the harmonic vibrational frequencies were computed analytically.

Results

Matrix-isolation experiments using argon, neon, and hydrogen for laser-ablated Mo and DFT calculations of MoH_x species will be described.

Argon. The argon matrix reaction of laser-ablated Mo atoms and H_2 was investigated using 7 and 3.5 K substrate temperatures. The colder temperature trapped species more quickly and gave cleaner spectra with fewer aggregate absorptions. Important new absorptions at 1691.6, 1697.8, 1718.7 and 1761.9 cm^{-1} increased on photolysis and weak absorptions appeared at 1812.1 and 1857.6 cm^{-1} on annealing (Figure 1). The corresponding argon matrix experiments with D_2 gave the shifted bands listed in Table 1. An experiment with HD gave the same 1697.8 and 1218.4 cm^{-1} absorptions as H_2 and D_2 but different bands at 1726.8 and 1239.8 cm^{-1}.

Neon. An extensive series of experiments was done with 3, 4 and 6% H_2 in neon. The important sharp 1696.1, 1740.2, 1829.7, and 1882.0 cm^{-1} absorptions labeled MoH, MoH_2, MoH_4 and MoH_6 in Figure 2 display different annealing and photolysis behavior. Deuterium substitution gave the absorptions in Figure 3 as listed in Table 1. The reaction products with HD

* Author for correspondence. E-mail: lsa@virginia.edu.

10.1021/jp053591u CCC: $30.25
Published on Web 09/17/2005

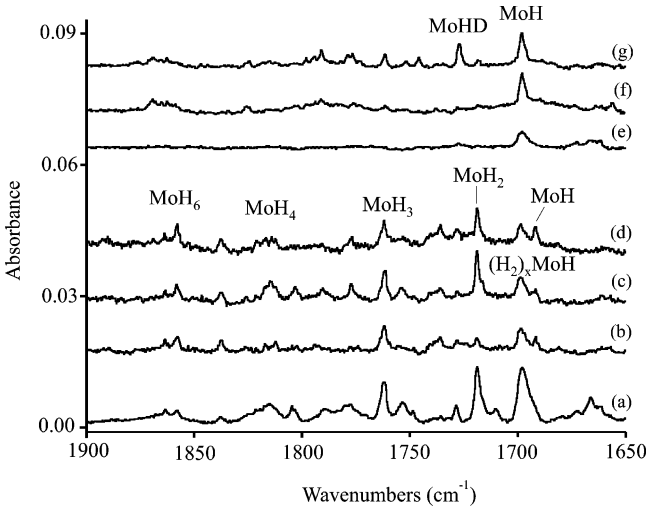

Figure 1. Infrared spectra in the 1900−1650 cm^{-1} region for laser-ablated Mo deposited with hydrogen in argon at 3.5 K. (a) 5% H_2 and Mo co-deposited for 1 h, (b) annealed to 15 K, (c) irradiated at 320−380 nm, and (d) annealed to 30 K. (e) 2% HD and Mo co-deposited for 1 h, (f) annealed to 30 K, and (g) irradiated at $\lambda > 220$ nm.

TABLE 1: Infrared Absorptions (cm^{-1}) Observed from Reactions of Laser-Ablated Mo Atoms and H_2 in Excess Argon, Neon, and Hydrogen

argon		neon		hydrogen		
H_2	D_2	H_2	D_2	H_2	D_2	identification
		1993.7				MoH_6
1857.6	1841.1	1882.0	1357.9			MoH_6
1812.1	1301.9	1829.7	1316.7			MoH_4
1761.9	1265.5	1773.6				
		1757	1263			
		1748				
1718.7	1234.2	1740.2	1250.6	1733.0	1247.1	MoH_2
1697.8		1704	1223		1220	$(H_2)_xMoH$
1691.6	1218.4	1696.1	1223			MoH
1637.0	1212.3	1619	1217.7		1137	Mo_xH_y
	1173.2		(1164)			
		966.2				$Mo(H_2)$?
		633.8	702.7	633.6	465.3	$(Mo(H_2)_x)$
			466.3			

give different absorptions for the higher bands, but the same absorptions at 1696.1 and 1217.7 cm^{-1}, as shown at the top of each figure. Finally, Figure 4 compares the spectra of group 6 metal atom and dihydrogen reaction products in solid neon.

Hydrogen and Deuterium. Molybdenum atoms were co-deposited with pure hydrogen, and the spectrum reveals strong absorptions at 1733.0 and 633.6 cm^{-1} as shown in Figure 5. These bands shifted to 1247.1 and 465.3 cm^{-1} in pure deuterium. Annealing, visible and ultraviolet photolysis gradually decrease the absorptions in both regions with more effect on the upper band. One experiment was done with 50% H_2 + 50% D_2, and the spectrum of the deposited sample is shown at the top of Figure 5. The upper bands shifted slightly to 1732.0 and 1263.6 cm^{-1} owing to different media, but notice that the hydrogen product is 20 times stronger than the deuterium product absorption. No mixed isotopic counterparts were observed for the lower product absorption. Finally, similar new experiments were done with tungsten and pure hydrogen. The hydrogen−tungsten spectrum reveals two strong bands at 1859.1 and 1830.2 cm^{-1}, counterparts to the 1334.0 and 1323.9 cm^{-1} pure deuterium−tungsten bands reported earlier.[16]

Calculations. DFT calculations were done with BPW91 and B3LYP functionals to provide a consistent set of frequencies for molybdenum hydrides. Previous SDCI calculations for MoH found a $^6\Sigma^+$ state with 1662 cm^{-1} harmonic frequency,[34] and more recent MRSDCI calculations determined a higher 1807 cm^{-1} harmonic frequency.[35] Our DFT calculations predict an intermediate frequency for MoH (Table 2). The BPW91 functional, 6-311++G(d,p) basis on hydrogen, and SDD pseudopotential and basis for Mo give a 1796 cm^{-1} frequency: The larger 6-311++G(3df,3pd) basis predicts 1791 cm^{-1} and the LANL2DZ pseudopotential for Mo gives the same results ±1 cm^{-1}. The B3LYP functional yields slightly lower frequencies at 1787 and 1775 cm^{-1} for the two pseudopotentials.

The Mo + H_2 reaction has been explored by MRSDCI calculations: Excited Mo(^{5}D, $4d^5 5s^2$) inserts spontaneously into H_2 to form bent MoH_2($^5B_2$, 116°, and 1.67 Å) and ground-state Mo(^{7}S) has a barrier (89 kcal/mol) to insertion.[36] Our DFT calculations for MoH_2 find a slightly longer bond and smaller angle (Table 3) and strong antisymmetric (b_2) stretching frequency (1826 cm^{-1}) and weaker symmetric (a_1) stretching frequency (1833 cm^{-1}) (BPW91). A previous DFT calculation at the LSDA level gave similar structural parameters and frequencies.[37]

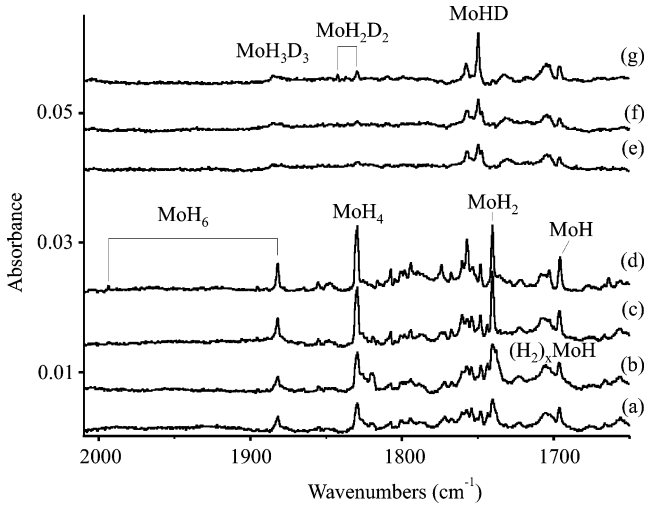

Figure 2. Infrared spectra in the 2010−1650 cm^{-1} region for laser-ablated Mo deposited with hydrogen in neon at 3.5 K. (a) 6% H_2 and Mo co-deposited for 1 h, (b) irradiated at 240−380 nm, (c) annealed to 9 K, and (d) annealed to 11 K. (e) 6% HD and Mo co-deposited for 1 h, (f) annealed to 7.5 K, and (g) annealed to 9.5 K.

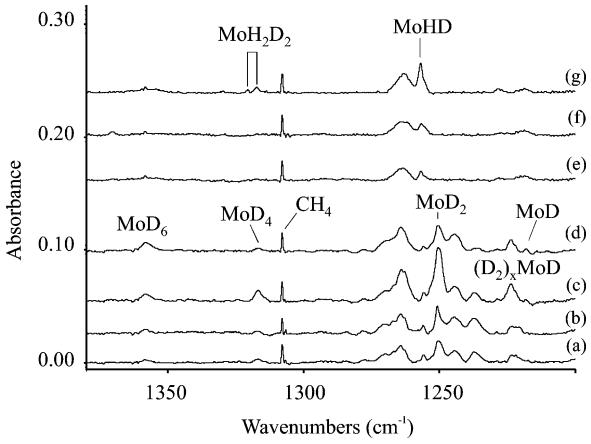

Figure 3. Infrared spectra in the 1380−1200 cm^{-1} region for laser-ablated Mo deposited with deuterium in neon at 3.5 K. (a) 6% D_2 and Mo co-deposited for 1 h, (b) irradiated at 240−380 nm, (c) annealead to 9 K, and (d) annealed to 11 K. (e) 6% HD and Mo co-deposited for 1 h, (f) annealed to 7.5 K, and (g) annealed to 9.5 K.

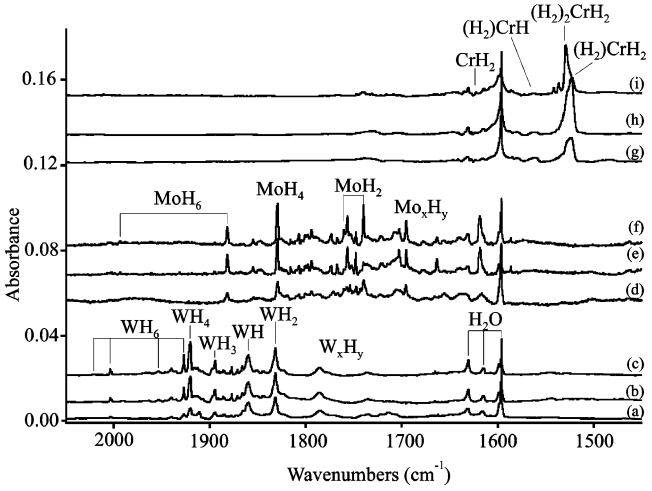

Figure 4. Infrared spectra in the 2050−1450 cm^{-1} region for laser-ablated group 6 metal atoms reacted with H_2 during condensation in excess neon at 3.5 K. (a) W and 4% H_2 co-deposited for 1 h in neon, (b) annealed to 10 K, and (c) annealed to 11 K. (d) Mo and 4% H_2 co-deposited for 1 h in neon, (e) annealed to 9 K, and (f) annealed to 11 K. (g) Cr and 5% H_2 co-deposited for 1 h in neon, (h) photolyzed at $\lambda > 290$ nm for 10 min, and (i) annealed to 12 K.

Recent CCSD(T) calculations on group 6 trihydrides find pyramidal (C_{3v}) molecules and predict an intense antisymmetric (e) fundamental at 1809 cm^{-1}.[38] Our DFT calculations for MoH_3 find a slightly higher frequency (1859 cm^{-1}) (BPW91) and provide mixed and all-D isotopic frequencies (Table 4). We note that the $^6A_1$ $(H_2)MoH$ complex structure is 9.8 kcal/mol higher energy than the $^4A_1$ MoH_3 ground state.

The MoH_4 molecule is found to be tetrahedral like WH_4 and unlike $(H_2)CrH_2$.[15−18] The two t_2 modes are calculated at 1889 and 523 cm^{-1} with relatively high intensities (Table 5). The lower symmetry CH_2D_2 molecule is predicted to exhibit four observable stretching modes.

Early calculations for MoH_6 and WH_6 found more relativistic contraction for the latter.[39] Although subsequent computations have focused on WH_6, Landis et al.[40] predicted sd^5 hybrid orbitals in MoH_6 with 64° and 116° angles, which is similar to the structure found for WH_6.[15−22] We have explored four MoH_6 structures and the bis $(H_2)_2MoH_2$ complex at the DFT level. Like WH_6, we find the distorted trigonal prism structure to be the global minimum energy with both density functionals (Table 6).

Discussion

The Mo + H_2 product absorptions will be assigned to MoH_x species on the basis of isotopic substitution and comparison of all matrix observations with DFT frequencies.

MoH. The 1697.8 cm^{-1} product absorption in solid argon decreases on annealing and shows little change on photolysis (Figure 1). This band shifts to 1218.4 cm^{-1} with D_2 (1.393 ratio) and both bands are unshifted with the HD reagent, which suggests a single H(D) atom vibration and assignment to a MoH species. The sharp weaker 1691.6 cm^{-1} band is resolved from the broader band on annealing and it sharpens and increases slightly on final annealing. These bands are probably due to MoH, but which one is isolated and which one is complexed by unreacted dihydrogen molecules? A thermal Mo/photochemical investigation at Rice[14] assigned a 1674.5 cm^{-1} absorption to MoH in solid krypton, which is compatible with the present argon matrix observation, considering the expected larger red shift in the more polarizable matrix host. The Rice group did not trap MoH in solid argon at 12 K. We believe 12 K is too high for argon to retain H_2 efficiently and to trap small molecules particularly in the light of a 2100−2300 °C Mo filament. The neon matrix experiments reveal a broad 1704 cm^{-1} band and a sharp 1696.1 cm^{-1} feature. The sharp 1696.1 cm^{-1} feature increases on annealing, shifts to 1217.7 cm^{-1} with D_2 (1.393 ratio), and both features appear unshifted with HD (Figures 2 and 3). Although one can reasonably expect MoH to react on annealing, the atoms could also react to form MoH itself on annealing. Hence, the sharp 1691.6 cm^{-1} band could be due to MoH in solid neon. If this were the case, the preferred argon matrix assignment would be the sharp lower band at 1691.6 cm^{-1}. The broader 1704 cm^{-1} band in solid neon is most likely due to an aggregate species, and the $(H_2)_xMoH$ complex is appropriate. Finally, our DFT calculations and the neon, argon and krypton matrix results extrapolate to a gas-phase MoH fundamental near 1720 ± 20 cm^{-1}.

MoH_2. Molybdenum dihydride complexes exhibit modes between 1647 and 1847 cm^{-1} depending on the ligands and the medium.[11,12] The only experimental evidence currently available for isolated MoH_2 is the Rice study,[14] which assigned strong 1709.3 cm^{-1} and medium intensity 1743.1 cm^{-1} absorptions to ν_3 (b_2) and ν_1 (a_1) of bent MoH_2 in solid krypton. In Figure 9 of the Rice paper, the 1743.1 cm^{-1} band varies from 25% to 100% of the 1709.1 cm^{-1} band on different photolysis exposures, which, we think casts doubt on assignment of both bands to the same product species. These workers report, but do not illustrate, 1752.7 and 1727.4 cm^{-1} argon matrix bands for MoH_2: Our 7 and 3.5 K argon matrix samples exhibit instead a 1718.7 cm^{-1} band, which, we believe, is the argon matrix counterpart of the 1709.3 cm^{-1} MoH_2 band in solid krypton. This assignment is supported by the D_2 observation at 1234.2 cm^{-1} (H/D isotopic ratio 1.393) and more importantly new 1726.8 and 1239.8 cm^{-1} bands with the HD reagent, which forms the HMoD molecule.[41] The absorptions of MoH_2 and MoD_2 in solid neon were observed slightly higher at 1740.5 and 1250.6 cm^{-1}, respectively (ratio 1.393). Again the HD counterparts at 1749.7 and 1256.8 cm^{-1} are above the b_2 modes of the pure isotopomers because the weaker a_1 modes are at still higher comparable wavenumbers, as predicted by our calculations.

Our assignments to MoH_2 are supported by DFT calculations, which predict ν_3 (b_2) near 1820 cm^{-1} (SDD, Table 3). The scale factor (observed neon matrix/calculated) = 1740.5/1825.9 = 0.953. On the basis of the krypton (1709.3 cm^{-1}) and argon (1718.7 cm^{-1}) matrix effects, we believe the gas-phase value will be near the neon matrix measurement (1740 ± 10 cm^{-1}). Finally, MoH_2 is a bent molecule based on electronic structure calculations and not on the now questioned observation of the ν_1 (a_1) mode.

MoH_3. No band in any of the matrix spectra commands assignment to MoH_3. If our BPW91 calculation (1859 cm^{-1}) for the strong ν_3 (e) mode is scaled by 0.953, a 1772 cm^{-1} neon matrix prediction results. The argon matrix will red shift this 10−20 cm^{-1} and the krypton matrix 10−20 cm^{-1} more, but not as low as the 1680 cm^{-1} band assigned by the Rice group.[14] Furthermore, our calculation for MoH_2D predicts the major absorption unshifted from MoH_3, and the 1680 cm^{-1} absorption shifts to 1676 cm^{-1}. We believe that the CCSD(T)[38] and DFT calculations cast doubt on the 1680 cm^{-1} krypton matrix assignment[14] to MoH_3. However, the 1743.1 cm^{-1} band first assigned to MoH_2 could be due to MoH_3. Our 1761.9 cm^{-1} argon matrix band, and the weak 1773.6 cm^{-1} neon matrix band, which grows on annealing, could be due to MoH_3.

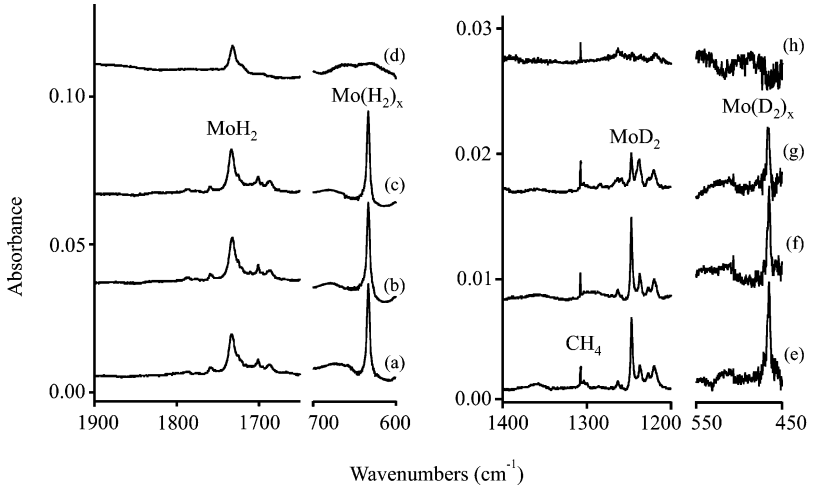

Figure 5. Infrared spectra for laser-ablated Mo deposited with solid molecular hydrogen at 3.5 K. (a) H_2 co-deposited for 25 min, (b) annealed to 6 K, and (c) irradiated at 240−380 nm. (d) $H_2 + D_2$ co-deposited for 25 min. (e) D_2 co-deposited for 30 min, (f) annealed to 8 K, and (g) irradiated at $\lambda > 220$ nm. (h) $H_2 + D_2$ co-deposited for 25 min.

TABLE 2: Calculated Bond Lengths, Vibrational Frequencies, and Infrared Intensities for MoH

method	state, bond (Å)	frequencies, cm^{-1} (intensities, km/mol)
BPW91/6-311++G(d,p)/SDD	$^6\Sigma^+$, 1.714	MoH: 1796.0 (165) MoD: 1277.2 (83)
BPW91/6-311++G(3df,3pd)/SDD	$^6\Sigma^+$, 1.711	MoH: 1791.2 (157) MoD: 1273.8 (80)
BPW91/6-311++G(d,p)/LanL2DZ	$^6\Sigma^+$, 1.708	MoH: 1797.3 (211) MoD: 1278.1 (107)
BPW91/6-311++G(3df,3pd)/LanL2DZ	$^6\Sigma^+$, 1.711	MoH: 1791.0 (196) MoD: 1273.6 (99)
B3LYP/6-311++G(d,p)/SDD	$^6\Sigma^+$, 1.719	MoH: 1787.0 (232) MoD: 1270.8 (118)
B3LYP/6-311++G(d,p)/Lanl2DZ	$^6\Sigma^+$, 1.715	MoH: 1774.9 (279) MoD: 1262.1 (141)

TABLE 3: Calculated Geometries, Vibrational Frequencies, and Infrared Intensities for MoH_2 ($^5B_2$, C_{2v})

method	geometry (Å, deg)	frequencies, cm^{-1} (modes, intensities, km/mol)
BPW91/6-311++G(d,p)/SDD	MoH: 1.708 HMoH: 109.5	MoH_2: 1833.3 (a_1, 85), 1825.9 (b_2, 249), 569.6 (a_1, 96) MoD_2: 1301.7 (a_1, 44), 1300.7 (b_2, 128), 405.6 (a_1, 49) MoHD: 1829.8 (166), 1301.2 (87), 493.7 (76)
BPW91/6-311++G(d,p)/Lanl2DZ	MoH: 1.701 HMoH: 106.4	MoH_2: 1833.0 (a_1, 99), 1799.7 (b_2, 269), 515.5 (a_1, 110) MoD_2: 1301.6 (a_1, 51), 1281.7 (b_2, 138), 367.0 (a_1, 56) MoHD: 1816.9 (181), 1291.3 (98), 447.1 (87)
B3LYP/6-311++G(d,p)/SDD	MoH: 1.71 HMoH: 108.8	MoH_2: 1830.1 (a_1, 124), 1818.8 (b_2, 336), 571.9 (a_1, 110) MoD_2: 1299.6 (a_1, 64), 1295.5 (b_2, 172), 407.2 (a_1, 56) MoHD: 1824.6 (227), 1297.7 (121), 495.8 (87)
B3LYP/6-311++G(d,p)/Lanl2DZ	MoH: 1.70 HMoH: 105.1	MoH_2: 1830.8 (a_1, 135), 1795.1 (b_2, 353), 530.7 (a_1, 117) MoD_2: 1300.3 (a_1, 70), 1278.3 (b_2, 180), 377.8 (a_1, 59) MoHD: 1813.5 (239), 1288.9 (131), 460.5 (94)

MoH_4. The sharp 1829.7 cm^{-1} absorption increases on annealing and photolysis in the neon matrix experiments in a manner parallel to WH_4,[16] and the 1829.7 cm^{-1} band is assigned to ν_3 (t_2) of tetrahedral MoH_4. This band shifts to 1316.7 cm^{-1} with D_2 (isotopic frequency ratio 1.390) and exhibits four bands at 1842.6, 1829.7, 1320.9, and 1317.1 cm^{-1} with HD. Our BPW91 calculation predicts the ν_3 (t_2) mode for MoH_4 at 1889 cm^{-1}, and a 0.969 scale factor will fit the calculation to the observed band. Further DFT calculations show that the t_2 modes of MoH_4 and MoD_4 are split into unshifted b_2 and blue shifted a_1 counterparts in MoH_2D_2 (Table 5). The BPW91 calculation predicts a 13.1 cm^{-1} splitting for the Mo−H_2 stretching modes and a 4.2 cm^{-1} splitting for the Mo-D_2 modes in MoH_2D_2. The neon matrix observed splittings are 12.9 and 3.8 cm^{-1}, which is excellent agreement for this diagnostic isotopic shift.

Our BPW91 calculation also predicts the $\nu_4(t_2)$ bending mode of MoH_4 at 523 cm^{-1} with 70% of the intensity of ν_3 (t_2). A sharp band at 487.2 cm^{-1} tracks with the 1829.7 cm^{-1} absorption and exhibits 50% of its IR intensity. The 487.2 cm^{-1} band is assigned to ν_4 of MoH_4. The scale factor 0.932 is slightly less for ν_4 than the 0.969 value for ν_3.

In our argon matrix experiments, 1812.1 and 1301.9 cm^{-1} frequencies are counterpart to the above neon matrix bands for MoH_4.

MoH_6. The sharp 1882.0 cm^{-1} neon matrix absorption increases on annealing, decreases on photolysis, and increases on final annealing when MoH_4 decreases slightly and MoH_2

TABLE 4: Calculated Geometries, Vibrational Frequencies, and Infrared Intensities for MoH_3 ($^4A_1$, C_{3v})

molecule	geometry	relative energy (kcal/mol)	frequencies, cm^{-1} (modes, intensities, km/mol)
			BPW91/6-311++G(d,p)/SDD
MoH_3 ($^4A_1$, C_{3v})	MoH: 1.703 HMoH: 109.4	0.0	MoH_3: 1876.3 (a_1, 30), 1858.7 (e, 229 × 2), 634.5 (e, 62 × 2), 410.1 (a_1, 170) MoD_3: 1329.8 (a_1, 16), 1324.3 (e, 119 × 2), 451.2 (e, 31 × 2), 294.0 (a_1, 87) MoH_2D: 1870.6 (95), 1858.9 (227), 1326.3 (88), 634.8 (70), 533.3 (35), 374.7 (143) $MoHD_2$: 1864.8 (160), 1327.9 (52), 1324.4 (121), 568.3 (58), 470.4 (30), 333.1 (112)
$(H_2)MoH$ ($^6A_1$, C_{2v})	MoH: 1.739 MoH′: 2.201 H′H′: 0.776	9.8	3881.4 (a_1, 56), 1755.2 (a_1, 255), 835.7 (b_2, 8), 497.4 (a_1, 3), 331.2 (b_1, 28), 309.4 (b_2, 41)
			B3LYP/6-311++G(d,p)/SDD
MoH_3 ($^4A_1$, C_{3v})	MoH: 1.704 HMoH: 108.2	0.0	MoH_3: 1893.1 (a_1, 44), 1867.2 (e, 306 × 2), 622.8 (e, 63 × 2), 423.6 (a_1, 200) MoD_3: 1342.1 (a_1, 23), 1330.3 (e, 158 × 2), 442.7 (e, 32 × 2), 303.6 (a_1, 103) MoH_2D: 1884.7 (128), 1867.3 (304), 1334.4 (120), 612.4 (73), 524.6 (34), 386.2 (169) $MoHD_2$: 1876.0 (213), 1338.1 (72), 1330.5 (161), 556.4 (61), 464.3 (32), 342.4 (130)
$(H_2)_2MoH$ ($^6A_1$, C_{2v})	MoH: 1.746 MoH′: 2.218 H′H′: 0.767	10.7	4038.1 (a_1, 33), 1740.2 (a_1, 308), 845.5 (b_2, 8), 486.4 (a_1, 3), 332.8 (b_1, 42), 315.7 (b_2, 57)

TABLE 5: Calculated Geometries, Vibrational Frequencies, and Intensities for MoH_4 and $(H_2)MoH_2$

molecule	geometry (Å, deg)	relative energy (kcal/mol)	frequencies, cm^{-1} (modes, intensities, km/mol)
			BPW91/6-311++G(d,p)/SDD
MoH_4 ($^3A_1$, T_d)	MoH: 1.697	0.0	MoH_4: 1915.2 (a_1, 0), 1889.0 (t_2, 202 × 3), 674.4 (e, 0 × 2), 523.0 (t_2, 140 × 3) MoD_4: 1354.8 (a_1, 0), 1346.1 (t_2, 107 × 3), 477.0 (e, 0 × 2), 374.0 (t_2, 72 × 3) MoH_2D_2: 1902.3 (98), 1889.2 (201), 1350.4 (56), 1346.2 (109), 619.3 (38), 583.1 (0), 488.3 (122), 415.0 (89), 404.7 (68)
$(H_2)MoH_2$ ($^5B_2$, C_{2v})	MoH: 1.698 MoH′: 2.193 H′H′: 0.781 HMoH: 71.0	16.6	$(H_2)MoH_2$: 3806.8 (a_1, 134), 1868.1 (a_1, 145), 1838.1 (b_2, 102), 840.8 (b_1, 7), 577.2 (a_1, 4), 487.8 (a_1, 0), 428.8 (a_1, 22), 236.0 (b_1, 60), 153.4i (b_2, 55).
			B3LYP/6-311++G(d,p)/SDD
MoH_4 ($^3A_1$, T_d)	MoH: 1.695	0.0	MoH_4: 1942.4 (a_1, 0), 1909.8 (t_2, 271 × 3), 702.6 (e, 0 × 2), 534.3 (t_2, 148 × 3) MoD_4: 1374.0 (a_1, 0), 1361.0 (t_2, 142 × 3), 497.0 (e, 0 × 2), 382.8 (t_2, 76 × 3) MoH_2D_2: 1926.4 (131), 1909.9 (268), 1367.4 (76), 1361.3 (146) 643.1 (38), 607.8 (0), 499.9 (129), 425.1 (94), 415.6 (73)
$(H_2)MoH_2$ ($^5B_2$, C_{2v})	MoH. MoH′: H′H′: HMoH:	13.7	$(H_2)MoH_2$: 4416.1 (a_1, 0), 1832.6 (a_1, 126), 1821.2 (b_2, 336), 569.7 (a_1, 110), 110.9 (b_1, 0), 12.0 (a_1, 0), 18.0i (a_2, 0), 91.3i (b_2, 52), 144.8i (b_1, 163)

decreases markedly. The 1882.0 cm^{-1} band shifts to 1357.9 cm^{-1} with D_2 (ratio 1.386), and to 1885.1 cm^{-1} with HD. A weaker 1993.7 cm^{-1} band (15% as intense) tracks with the 1882.0 cm^{-1} absorption. The 1882.0 and 1357.9 cm^{-1} absorptions increase on late annealing when the MoH_4/MoD_4 absorptions decrease, hence the MoH_6 identification must be considered. In addition, the 1882.0, 1993.7 cm^{-1} bands (Figure 4) follow the behavior of the WH_6 absorptions.[16]

The 1882.0 and 1993.7 cm^{-1} absorptions fit the two strongest Mo−H stretching modes (e) of the global minimum trigonal prism structure for MoH_6 (Table 6) using identical 0.984 scale factors. The above bands do not fit the frequency-intensity pattern calculated for the C_{5v} parachute structure, but the observed bands are compatible with the C_{3v} hemisphere pattern using 0.970, 0.967 scale factors. The latter structure is 3.3 kcal/mol higher at the BPW91 level and 5.9 kcal/mol higher at the B3LYP level. We favor the C_{3v} prism structure for MoH_6, the structure computed for WH_6,[20−22] as described in a recent review,[25] but we cannot rule out the C_{3v} hemisphere for MoH_6 with only two observed Mo−H stretching frequencies. In the WH_6 case the observation of four W−H stretching frequencies, and the a_1, e, a_1, e pattern provided solid evidence for the distorted C_{3v} prism structure.[15,16]

The 1885.1 cm^{-1} band observed with HD is due to the MoH_3 (long bond) D_3 (short bond) isomer, which is the global minimum for this isotope from zero point energy (by 0.3 kcal/mol over MoH_3 (short bond) D_3 (long bond)). This suggests that HD adds preferentially to MoH_2D_2 to give the slightly more stable MoH_3 (long bond) D_3 (short bond) isomer. (See Figure 6 for the orientation of long and short Mo−H bonds.)

Other Absorptions. As in the tungsten experiments,[16] other absorptions cannot be assigned. Many of these are broad (1724, 1705, 1619 cm^{-1} in neon) and they remain on annealing. These bands are probably due to higher metal cluster hydride species.

Dihydrogen Complex. The sharp 633.6 cm^{-1} band in solid hydrogen shifts to 465.3 cm^{-1} in solid deuterium, which define a 1.362 H/D ratio. The position and low H/D ratio for this band are near that observed for the $Pd(H_2)_3$ dihydrogen complex at 730 cm^{-1} and 1.33.[42] Neon matrix counterparts were observed at 633.8 and 466.3 cm^{-1}. Unfortunately, mixed isotopic components could not be observed presumably due to isotopic dilution. We tentatively assign the 633 cm^{-1} band to a higher $Mo(H_2)_n$ dihydrogen complex. Such a species is unique to molybdenum in Group 6 as a tungsten counterpart was not observed. However, ongoing studies with Pd in solid hydrogen show only the higher dihydrogen complex.

The 966.2 cm^{-1} band with H_2 in solid neon increased on annealing, but only a weak D_2 counterpart was observed at 702.7 cm^{-1} (ratio 1.375), and no HD counterpart was found.

TABLE 6: Calculated Geometries, Vibrational Frequencies, and Intensities for MoH_6[a]

molecule (state, symmetry)	geometry (Å, deg)	relative energy (kcal/mol)	frequencies, cm^{-1} (modes, intensities/km/mol)
MoH_6 (prism)[b] ($^1A_1$, C_{3v})	MoH: 1.691 MoH′: 1.646 HMoH: 117.0 H′MoH′: 61.1	0.0	2051.6 (a_1, 46), 2025.7 (e, 54 × 2), 1916.3 (a_1, 73), 1913.0 (e, 158 × 2), 1103.7 (a_1, 110), 933.8 (e, 72 × 2), 875.3 (e, 38 × 2), 761.7 (a_2, 0), 727.1 (e, 0 × 2), 713.7 (a_1,12)
MoH_6 (parachute) ($^1A_1$, C_{5v})	MoH: 1.717 MoH′: 1.662 HMoH′: 116.3	2.1	1995.5 (e_1, 172 × 2), 1993.8 (a_1, 36), 1951.1 (e_2, 0 × 2), 1871.5 (a_1, 198), 999.7 (e_2, 0 × 2), 949.5 (a_1, 0), 908.5 (e_1, 125 × 2), 746.9 (e_1, 0 × 2), 717.1 (e_2, 0 × 2)
MoH_6 (hemisphere) ($^1A_1$, C_{3v})	MoH: 1.677 MoH′: 1.635 HMoH: 116.7 H′MoH′: 62.4	3.3	2081.8 (a_1, 16), 2060.9 (e, 45 × 2), 1940.0 (e, 157), 1930.3 (a_1, 26), 1126.3 (a_1, 123), 1083.8 (e, 152 × 2), 919.8 (e, 28 × 2), 759.1 (e, 2 × 2), 712.2 (a_1, 33), 596.9 (a_2, 0)
MoH_6 (umbrella) ($^1A_1$, C_{5v})	MoH: 1.627 MoH′: 1.653 HMoH′: 63.5	7.7	2112.8 (a_1, 6), 2009.8 (e_1, 200), 2002.0 (a_1, 0), 1964.0 (e_2, 0 × 2), 1111.7 (e_2, 262 × 2), 1076.1 (a_1, 38), 1074.3 (e_2, 0), 672.9 (e_1, 0 × 2), 672.0 (e_2, 0 × 2)
$(H_2)_2MoH_2$ ($^3A''$, C_s)	1.696, 117.0°, 1.829, 0.884	13.4	2651 (a′, 0), 2532 (a″, 909), 1882.1 (a′, 59), 1881.7 (a′, 283), 1760 (a′, 20), ...
MoH_6 (prism)[b] ($^1A_1$, C_{3v})	MoH: 1.690 MoH′: 1.641 HMoH: 116.5 H′MoH′: 61.6	0.0	2086.7 (a_1, 52), 2052.5 (e, 78 × 2), 1945.7 (a_1, 99), 1933.0 (e, 194 × 2), 1121.9 (a_1, 137), 929.6 (e, 86 × 2), 856.1 (e, 42 × 2), 788.6 (a_2, 0), 730.9 (a_1, 4), 712.9 (e, 0 × 2)
MoH_6 (parachute) ($^1A_1$, C_{5v})	MoH: 1.715 MoH′: 1.658 HMoH′: 116.1	1.5	2032.3 (a_1, 41), 2028.0 (e_1, 215 × 2), 1971.2 (e_2, 0 × 2), 1906.8 (a_1, 265), 1003.6 (e_2, 0 × 2), 950.7 (a_1, 0), 902.3 (e_1, 143 × 2), 756.5 (e_1, 0 × 2), 711.4 (e_2, 0 × 2)
MoH_6 (umbrella) ($^1A_1$, C_{5v})	MoH: 1.619 MoH′: 1.651 HMoH′: 64.1	11.7	2149.7 (a_1, 6), 2031.6 (e_1, 253 × 2), 2025.9 (a_1, 0), 1972.1 (e_2, 0 × 2), 1103.3 (e_1, 312 × 2), 1077.0 (e_2, 0 × 2), 1072.5 (a_1, 31), 665.9 (e_1, 1 × 2), 649.1 (e_2, 0 × 2)
MoH_6 (hemisphere) ($^1A_1$, C_{3v})	MoH: 1.679 MoH′: 1.629 HMoH: 117.5 H′MoH′: 62.1	5.9	2117.9 (a_1, 17), 2090.2 (e, 57 × 2), 1948.7 (e, 202 × 2), 1941.7 (a_1, 38), 1135.8 (a_1, 135), 1083.4 (e, 185 × 2), 892.3 (e, 30 × 2), 771.7 (e, 2 × 2), 713.1 (a_1, 49), 542.7 (a_2, 0)
$(H_2)_2MoH_2$ ($^3A''$, C_s)	1.699, 115.8°, 1.853, 0.847	7.4	2977 (a′, 1), 2859 (a″, 1052), 1882 (a′, 87), 1876 (a′, 394), 1718 (a′, 28), ...[c]

[a] Top section is BPW91, bottom section is B3LYP, both used 6-311++G(d,p) and SDD. [b] C_{3v} prism is global minimum energy structure. [c] Only higher frequencies are given for the bis complex.

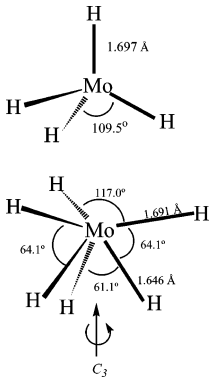

Figure 6. Structures of MoH_4 and MoH_6 computed at the BPW91/611++G(d,p)/SDD level of theory.

This is the region for M−(H_2) stretching modes,[1−3,10,42] and the simple Mo(H_2) complex is possible, but without more evidence this too must be considered tentative. This simple complex was not observed in solid hydrogen as a higher complex must be formed.

Products in Solid Hydrogen Matrixes. The strong band at 1733.0 cm^{-1} with Mo in pure H_2 falls in line with the 1740.2 and 1718.7 cm^{-1} neon and argon matrix counterparts for MoH_2. The 1733.0/1247.1 = 1.390 ratio is essentially the same as observed for MoH_2/MoD_2 in solid neon and argon; hence MoH_2 is not suffering significant perturbation by the pure hydrogen matrix molecules. More surprising is the fact that MoH_2 does not react with the H_2 matrix to form MoH_4 and MoH_6 as clearly happens in the solid neon, argon, and krypton[14] media. Almost the same situation was found here for W in pure H_2: Strong bands were observed for WH and WH_2 within 1 cm^{-1} of their neon matrix values, but only a weak band was observed at 1911 cm^{-1} for [WH_4] in solid hydrogen.

Reaction Mechanisms. The insertion of ground-state molybdenum into dihydrogen to form MoH_2, reaction 1, is exothermic by 9.0 kcal/mol at the BPW91 level and by 6.9 kcal/mol at the MRSDCI level.[36] However, the latter calculations predicted an 89 kcal/mol barrier for insertion by Mo(^{7}S) but a spontaneous reaction for excited Mo(b^5D, $4d^5\ 5s^1$). Xiao et al. found that 320−380 nm irradiation initiated the reaction of Mo and H_2 in solid krypton.[14] In our experiments MoH_2 was formed on deposition with laser-ablated atoms, which are known to contain excess kinetic/electronic energy, and MoH_2 did not increase on initial annealing to allow diffusion of trapped species, but MoH_2 did increase on ultraviolet photolysis. In addition, H atoms are produced in the deposition process so that metal atom-hydrogen atom combination can occur.

$$Mo(^7S) + H_2\ (^1\Sigma_g^+) \rightarrow MoH_2\ (^5B_2) \qquad \Delta E = -9.0\ \text{kcal/mol} \quad (1)$$

$$MoH_2\ (^5B_2) + H_2\ (^1\Sigma_g^+) \rightarrow MoH_4\ (^3A_1) \qquad \Delta E = -14.3\ \text{kcal/mol} \quad (2)$$

$$MoH_4\ (^3A_1) + H_2\ (^1\Sigma_g^+) \rightarrow MoH_6\ (^1A_1) \qquad \Delta E = -10.1\ \text{kcal/mol} \quad (3)$$

$$MoH\ (^6\Sigma) + H_2\ (^1\Sigma_g^+) \rightarrow MoH_3\ (^4A_1) \qquad \Delta E = -11.4\ \text{kcal/mol} \quad (4)$$

The MoH_2 molecule reacts spontaneously with H_2 to form MoH_4

and MoH_6, reactions 2 and 3. (Reaction energies are from BPW91 calculations, which are in accord with earlier results.[43]) The Mo reaction with H_2 is also exothermic, and MoH produced in the initial reaction can so react to form MoH_3.

The major difference among Cr, Mo and W reactions with pure $H_2(D_2)$ is that the major chromium product is red-shifted nearly 100 cm^{-1} from CrH_2 in neon and is thus identified as the $(H_2)_2CrH_2$ complex but that the Mo and W products are within a few cm^{-1} of isolated $MoH_2(MoD_2)$ and $WH_2(WD_2)$ in solid neon. This suggests that super dihydrogen complexes of MoH_2 and WH_2 are formed in pure solid hydrogen, which prevents the reaction of one and two H_2 molecules to give the higher hydride MoH_4 and MoH_6 molecules that are observed in solid neon.

Conclusions

Laser-ablated Mo atoms react with H_2 upon condensation in excess argon, neon, and pure hydrogen at 3.5 K. The molybdenum hydrides MoH, MoH_2, MoH_4, and MoH_6 are identified by the effects of isotopic substitution (H_2, D_2, HD, $H_2 + D_2$) and different matrix hosts on the infrared spectra and by comparison with vibrational frequencies calculated by density functional theory. The MoH_2 molecule is bent, MoH_4 is tetrahedral, as found for WH_2 and WH_4, and MoH_6 appears to have the same distorted trigonal prism structure found by matrix infrared spectroscopy and theory for WH_6.[16] Overall, Mo appears to be less reactive than W with hydrogen molecules.

Acknowledgment. We gratefully acknowledge support from NSF Grant CHE 03-52487.

References and Notes

(1) Kubas, G. J.; Ryan, R. R.; Swanson, B. I.; Vergamini, P. J.; Wasserman, H. J. *J. Am. Chem. Soc.* **1984**, *106*, 451.
(2) Sweany, R. L. *J. Am. Chem. Soc.* **1985**, *107*, 2374.
(3) Kubas, G. J. *Acc. Chem. Res.* **1988**, *21*, 120.
(4) Upmacis, R. K.; Poliakoff, M.; Turner, J. J. *J. Am. Chem. Soc.* **1986**, *108*, 3645.
(5) Crabtree, R. H.; Lavin, M. *J. Chem. Soc., Chem. Commun.* **1985**, 794.
(6) Heinekey, D. M.; Oldham, W. J. *Chem. Rev.* **1993**, *93*, 913.
(7) Walsh, E. F.; Popov, V. K.; George, M. W.; Poliakoff, M. *J. Phys. Chem.* **1995**, *99*, 12016.
(8) Geoff, S. E.; Nolan, T. F.; George, M. W. Poliakoff, M. *Organometallics* **1998**, *17*, 2730.
(9) Esteruelas, M. A.; Oro, L. A. *Chem. Rev.* **1998**, *98*, 577.
(10) Kubas, G. J. Metal Dihydrogen and σ-Bond Complexes. In *Modern Inorganic Chemistry*; Fackler, J. P., Jr., Ed.; Kluwer Academic/Plenum Publishers: New York, 2001 (see also references therein). See also: Bender, B. R.; Kubas, G. J.; Jones, L. H.; Swanson, B. I.; Eckert, J.; Capps, K. B.; Hoff, C. D *J. Am. Chem. Soc.* **1997**, *119*, 9179.
(11) Geoffrey, G. L.; Bradley, M. G. *Inorg. Chem.* **1978**, *17*, 2410.
(12) Kubas, G. J.; Ryan, R. R.; Unkefer, C. J. *J. Am. Chem. Soc.* **1987**, *109*, 8113.
(13) Van Zee, R. J.; DeVore, T. C.; Weltner, W., Jr. *J. Chem. Phys.* **1979**, *71*, 2051.
(14) Xiao, Z. L.; Hauge, R. H.; Margrave, J. L. *J. Phys. Chem.* **1992**, *96*, 636.
(15) Wang, X.; Andrews, L. *J. Am. Chem. Soc.* **2002**, *124*, 5636.
(16) Wang, X.; Andrews, L. *J. Phys. Chem. A* **2002,** *106*, 6720.
(17) Wang, X.; Andrews, L. *J. Phys. Chem. A* **2003,** *107*, 570.
(18) (a) Deleeuw, B. J.; Yamaguchi, Y.; Schaefer, H. F., III. *Mol. Phys.* **1995**, *84*, 1109. (b) Ma, B.; Collins, C. L.; Schaefer, H. F., III. *J. Am. Chem. Soc.* **1996**, *118*, 870.
(19) (a) Kang, S. K.; Albright, T. A.; Eisenstein, O. *Inorg. Chem.* **1989**, *28*, 1611. (b) Kang, S. K.; Tang, H.; Albright, T. A. *J. Am. Chem. Soc.* **1993**, *115*, 1971.
(20) Shen, M.; Schaefer, H. F., III; Partridge, H. *J. Chem. Phys.* **1993**, *98*, 508.
(21) (a) Tanpipat, N.; Baker, J. *J. Phys. Chem.* **1996**, *100*, 19818. (b) Landis, C. R.; Cleveland, T.; Firman, T. K. *J. Am. Chem. Soc.* **1998**, *120*, 2641.
(22) (a) Kaupp, M. *J. Am. Chem. Soc.* **1996**, *118*, 3018. (b) Kaupp, M. *Angew. Chem., Int. Ed. Engl.* **2001**, *40*, 3534. (c) Straka, M.; Hroberik, P.; Kaupp, M. *J. Am. Chem. Soc.* **2005**, *127*, 2591.
(23) Burkholder, T. R.; Andrews, L. *J. Chem. Phys.* **1991**, *95*, 8697.
(24) Hassanzadeh, P.; Andrews, L. *J. Phys. Chem.* **1992**, *96*, 9177.
(25) Andrews, L. *Chem. Soc. Rev.* **2004**, *33*, 123.
(26) Frisch, M. J.; Trucks, G. W.; Schlegel, H. B.; Scuseria, G. E.; Robb, M. A.; Cheeseman, J. R.; Zakrzewski, V. G.; Montgomery, J. A., Jr.; Stratmann, R. E.; Burant, J. C.; Dapprich, S.; Millam, J. M.; Daniels, A. D.; Kudin, K. N.; Strain, M. C.; Farkas, O.; Tomasi, J.; Barone, V.; Cossi, M.; Cammi, R.; Mennucci, B.; Pomelli, C.; Adamo, C.; Clifford, S.; Ochterski, J.; Petersson, G. A.; Ayala, P. Y.; Cui, Q.; Morokuma, K.; Malick, D. K.; Rabuck, A. D.; Raghavachari, K.; Foresman, J. B.; Cioslowski, J.; Ortiz, J. V.; Stefanov, B. B.; Liu, G.; Liashenko, A.; Piskorz, P.; Komaromi, I.; Gomperts, R.; Martin, R. L.; Fox, D. J.; Keith, T.; Al-Laham, M. A.; Peng, C. Y.; Nanayakkara, A.; Gonzalez, C.; Challacombe, M.; Gill, P. M. W.; Johnson, B.; Chen, W.; Wong, M. W.; Andres, J. L.; Gonzalez, C.; Head-Gordon, M.; Replogle, E. S.; Pople, J. A. *Gaussian 98*, revision A.6; Gaussian, Inc.: Pittsburgh, PA, 1998.
(27) Becke, A. D. *Phys. Rev. A* **1988**, *38*, 3098.
(28) Perdew, J. P.; Wang, Y. *Phys. Rev. B* **1992,** *45*, 13244.
(29) Becke, A. D. *J. Chem. Phys.* **1993**, *98*, 5648.
(30) Lee, C.; Yang, E.; Parr, R. G. *Phys. Rev. B* **1988**, *37*, 785.
(31) (a) Krishnan, R.; Binkley, J. S.; Seeger, R.; Pople, J. A. *J. Chem. Phys.* **1980**, *72*, 650. (b) Frisch, M. J.; Pople, J. A.; Binkley, J. S. *J. Chem. Phys.* **1984**, *80*, 3265.
(32) (a) Wadt, W. R.; Hay, P. J. *J. Chem. Phys.* **1985**, *82*, 284. (b) Hay, P. J.; Wadt, W. R. *J. Chem. Phys.* **1985**, *82*, 299.
(33) Andrae, D.; Haussermann, U.; Dolg, M.; Stoll, H.; Preuss, H. *Theor. Chim. Acta* **1990**, *77*, 123.
(34) Langhoff, S. R.; Pettersson, L. G. M.; Bauschlicher, C. W. Jr.; Partridge, H. *J. Chem. Phys.* **1987**, *86*, 268.
(35) Balasubramanian, K.; Li, J. *J. Phys. Chem.* **1990**, *94*, 4415.
(36) Li, J.; Balasubramanian, K. *J. Chem. Phys.* **1990**, *94*, 545.
(37) Martinez, A.; Koster, A. M.; Salahub, D. R. *J. Phys. Chem. A* **1997**, *101*, 1541.
(38) Balabanov, N. B.; Boggs, J. E. *J. Phys. Chem. A* **2000**, *104*, 7370.
(39) Pyykko, P.; Snijders, J. G.; Baerends, E. J. *Chem. Phys. Lett.* **1981**, *83*, 432.
(40) Landis, C. R.; Cleveland, T.; Firman, T. K. *J. Am. Chem. Soc.* **1995**, *117*, 1859.
(41) The Mo−H stretching mode of MoHD should be the average of the a_1 and b_2 stretching modes of MoH_2, and the Mo-D stretching mode of MoHD should be the average of the a_1 and b_2 modes of MoD_2 except where interaction forces the two MoHD modes further apart (see Table 3).
(42) Andrews, L.; Manceron, L.; Alikhani, M. E.; Wang, X. *J. Am. Chem. Soc.* **2000**, *122*, 11011.
(43) Siegbahn, P. E. M.; Blomberg, M. R. A.; Svensson, M. *J. Am. Chem. Soc.* **1993**, *115*, 4191.